Modeling and Simulating a Metamaterial to enhance Electromagnetic Power Transfer Efficiency

R. Barroso, W. Malpica, and A. Zozaya

***Abstract*—Several microwave power transfer efficiency applications involve interfaces where more than half of the incident wave's power density is frequently reflected. To enhance this efficiency, various media for impedance matching between volumetric materials used in biomedical, industrial, and environmental remediation applications have been proposed. However, they either exhibit high losses or require a specialized manufacturing process. Given that the use of volumetric metamaterials as matching media is an underexplored area of research, the authors of this paper first propose, model, and simulate a metallic cubic conductor metamaterial to investigate its understudied parameters. Then, the metamaterial is simulated in a quarter-wavelenght impedance transformer configuration to improve the efficiency of electromagnetic wave power transfer at an air-water interface. Numerical simulations and analytical modeling of this configuration show that the power density of the transmitted wave more than doubles respect to the interface without the proposed matching system. This improvement is achieved since the metamaterial has an intrinsic impedance within the same range as that of the materials to be matched, since the metamaterial is a low loss, a positively polarizable and exhibits a mu-near zero behaviour. In contrast to other impedance matching media, the suggested metamaterial has a low attenuation constant, offers a wide range of intrinsic impedance values, and can be constructed with readily available materials.**

Link to graphical and video abstracts, and to code: https://latamt.ieeer9.org/index.php/transactions/article/view/9532

***Index Terms*—MNZ, matching, absorber, microwave, WPT.**

I. Introduction

THE proper and efficient utilization of energy is a critical and increasingly important topic for many practical engineering applications. Among these, several heating, biomedical, telecommunications, radar, and wireless power transfer applications rely on microwave technology. By example, microwave heating is widely employed in industries such as chemicals [1] - [2], food [3] - [4], glass [5], mining [6], oil [7]- [8] and wood, [9]. This technique is also used for environmental thermoremediation of contaminated water and soils [6], [10]. Additionally, microwave hyperthermia has been applied in biomedical fields, such as cancer treatment [11]- [12]. In all these applications, enhancing the efficiency of microwave power transfer to the target substance is desirable.

Similar challenges arise in wireless communication and wireless power transmission (WPT), where improving energy efficiency is crucial for overcoming obstacles such as walls, reducing reflection losses [13]- [14].

A common solution to diminsh reflection losses involves the use of the impedance matching technique, which minimizes the reflection coefficient at the boundary between two different media. Initially developed for transmission lines [15], this technique has also been adapted for matching volumetric media at microwave frequencies, particularly in biomedical and industrial heating applications. However, the challenge of sourcing materials with the required electromagnetic properties has limited its widespread adoption.

In biomedical applications, such as microwave tomography and hyperthermia, liquid solutions have been used to match the impedance between biological tissues and air, or even directly between such tissues and radiant microwave antennas. Nevertheless, these liquid media have significant insertion losses due to Joule's efect [16], [17], [18]. In industrial heating, recent efforts have explored high-permittivity microwave ceramics as matching media between air and target materials [19]- [21]. Althoung promising, ceramic composites like Barium Titanate present challenges due to the specializated manufacturing process to ensure material homogeneity and precise control of its geometric and electromagnetic features, which limits their practical application [22]. These limitations highlight the need for more versatile, cost-effective solutions.

To address these challenges, a novel approach using two metasurfaces of rectangular conductor patches at an air/water interface was proposed for a water heating application in [23]. While this method demonstrated a slight increase in water temperature, it lacked a detailed explanation of the underlying electromagnetic impedance matching mechanism and the actual improvements in power transfer efficiency.

In response to these gaps, this paper presents a new approach utilizing a cubic conductor cells metamaterial as an impedance matching medium. Analytical and numerical models are developed to characterize critical aspects of the metamaterial´s behaviour. Unlike previous metamaterial studies [24], [25], the model introduced here quantifies the few studied intrinsic impedance, ohmic losses and frequency-dependent behavior of the metamaterial, providing a more comprehensive understanding of its advantages and limitations for the designing volumetric media for impedance matching systems. Compared to impedance matching liquids, the metamaterial exhibits a much lower attenuation constant.

The associate editor coordinating the review of this manuscript and approving it for publication was Pedro Moura (*Corresponding author: Raul Horacio Barroso*).

Raul Horacio Barroso is with the Electronic and Circuits Department, Simon Bolívar University, Miranda State, Venezuela (e-mail: rbarroso@usb.ve).

W. Malpica is with the Electrical Engineering School, Universidad Central de Venezuela, Caracas, Venezuela (e-mail: wilmer.malpica.ucv@gmail.com).

A. Zozaya is with Departamento de Electricidad, Universidad Tecnológica Metropolitana, Santiago, Chile (e-mail: a.zozayas@utem.cl).

Additionally, it can be fabricated from widely available and low-cost materials, provinding the metamaterial's property of reconfigurability, offering a broad range of intrinsic impedance values [26], unlike high-permittivity ceramics which are more difficult to source and own non-modifiable properties.

To demostrate the practical usefulness of this study, a quarter-wavelength impedance transformer slab based on the cubic conductor cells metamaterial is also designed for normal incidence at a plane interface. The analytical and simulation results demonstrate significant improvements in power transfer efficiency at an air-water interface when the impedance transformer slab is employed.

II. Materials and Methods

A. Background

1) Plane Waves in Transverse Electromagnetic Mode: A plane, harmonic and transverse electromagnetic (TEM) wave that propagates in an isotropic, linear and homogeneous medium of complex electric permittivity ϵ and complex magnetic permeability μ has electric field and a magnetic field associated to it, that are commonly defined as

$$\mathbf{E}(\mathbf{r}) = \hat{\mathbf{e}}\mathrm{E}_0 e^{-\gamma\hat{\mathbf{n}}\cdot\mathbf{r}} \tag{1}$$

$$\mathbf{H}(\mathbf{r}) = \hat{\mathbf{h}}\mathrm{H}_0 e^{-\gamma\hat{\mathbf{n}}\cdot\mathbf{r}} = \hat{\mathbf{n}} \times (\hat{\mathbf{e}}\mathrm{E}_0/\eta) e^{-\gamma\hat{\mathbf{n}}\cdot\mathbf{r}} \tag{2}$$

where $\hat{\mathbf{n}}$ is the unitary vector in the direction of propagation of the wave, E_0 and H_0 are vectorial fasor constants and, $\hat{\mathbf{e}}$ and $\hat{\mathbf{h}}$ are unitary vectors. Also, it is commonly defined that

$$\gamma = j\omega\sqrt{\epsilon\mu} = \alpha + j\beta = \alpha + j\omega/v \tag{3}$$

$$\lambda = 2\pi/\beta \tag{4}$$

$$\delta = 1/\alpha \tag{5}$$

$$\eta = \sqrt{\mu/\epsilon} \tag{6}$$

where γ is the wave propagation constant, α is the wave attenuation constant for $\alpha = \Re[\gamma]$, β is the wave phase constant for $\beta = \Im[\gamma] = 2\pi/\lambda$, λ is the wavelength in the medium, δ is the skin depth in the medium, η is intrinsic impedance of the medium while and ω is the wave angular frequency given by $\omega = 2\pi f$. Nevertheless, the complex electric permittivity is commonly defined as $\epsilon = \epsilon' - j\epsilon''$, where ϵ' is proportional to the medium polarizability and ϵ'' represent the medium electrical losses. In the same way, $\mu = \mu' - j\mu''$ where μ' is proportional to the medium magnetizability and μ'' represent the medium magnetic losses [27], [28]- [31]. It is also known that the average active power density vector $\bar{\mathbf{P}}(\mathbf{r})$ associated to the wave is given by

$$\bar{\mathbf{P}}(\mathbf{r}) = \frac{1}{2}\Re[\mathbf{E}(\mathbf{r}) \times \mathbf{H}(\mathbf{r})^*] = P_0 e^{-2\alpha\hat{\mathbf{n}}\cdot\mathbf{r}}\hat{\mathbf{n}} \tag{7}$$

being $P_0 = \Re\left[|\mathbf{E}_0|^2/2\eta^*\right]$.

2) The Power Transference for the Normal Incidence Case: For a problem of normal incidence [29], in which the incident wave propagates in the Medium 1 which is separated from the Medium 2 by the boundary of the $z = 0$ plane, there is presence of incident, reflected and transmitted waves that are represented in the Fig. 1, where the incident and reflected electric field amplitudes, as well as the incident and transmitted power vector amplitudes are related by the complex Fresnel coefficient Γ, as follows

$$\Gamma = \frac{E_{0r}}{E_{0i}} = \frac{\eta_2 - \eta_1}{\eta_2 + \eta_1} \tag{8}$$

$$P_{0t} = (1 - |\Gamma|^2) P_{0i} \tag{9}$$

Notice that the power transference efficiency in the interface is proportional to the value of $(1-|\Gamma|^2)$. If the condition $|\Gamma| = 0$ is achieved, $(1-|\Gamma|^2)$ is maximum and the interface between the two mediums is a perfectly matched one.

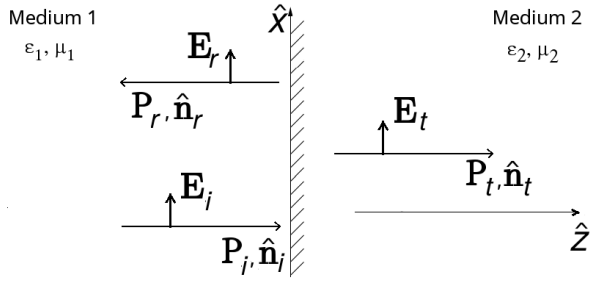

Fig. 1. A normal incidence case.

On the other hand, for a problem of normal incidence of a three layers media, as in Fig. 2, in which the incident wave propagates in the Medium 1 which is separated from the Medium M by a boundary on the $z = -d$ plane, and the Medium M is separated from the Medium 2 by another boundary on the $z = 0$ plane, the expressions of the reflection coefficients Γ_1 and Γ_m are both functions of the coordinate z [29].In order to compute them, the reflection coefficient in $z = 0^-$, let $\Gamma_m(0^-)$ is first calculated

$$\Gamma_m(0^-) = \frac{\eta_2 - \eta_m}{\eta_2 + \eta_m} \tag{10}$$

and then, the reflection coefficient along Medium M $\Gamma_m(z)$, is defined as

$$\Gamma_m(z) = \Gamma_m(0^-)\exp(2\gamma_m z) \tag{11}$$

Given the presence of the incident and reflected waves in the medium M, it is also useful to define a generalized impedance for the medium M, as a function of z

$$Z_m(z) = \eta_m \frac{1 + \Gamma_m(z)}{1 - \Gamma_m(z)} \tag{12}$$

Then, it is also calculated the reflection coefficient in the Medium 1 boundary on the $z = -d$ plane, let $\Gamma_1(-d^-)$

$$\Gamma_1(-d^-) = \frac{Z_m(-d) - \eta_1}{Z_m(-d) + \eta_1}. \tag{13}$$

Assuming that Medium 1 has negligible losses, a measure of the efficiency of the transference of power from the Medium

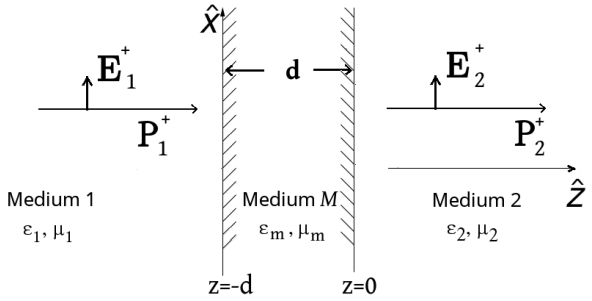

Fig. 2. Case of three media for normal incidence.

1 to the Medium 2 is given by $\mathcal{E}_{ff}$, where $\mathcal{E}_{ff} = {P_{02}}^+/{P_{01}}^+$ being P_{01}^+ the density power amplitude of the Medium 1 incident wave and, P_{02}^+ is the density power amplitude of the Medium 2 transmitted wave measured in $z = 0^+$. Then, assuming that the matching Medium M attenuation constant is α_m, that the net flow of density power in such medium is $P_m(z) = {P_m}^+ \exp(-2\alpha_m z) - {P_m}^- \exp(2\alpha_m z)$ and that such net flow of density power is continuous on the boundaries located on the planes $z = 0$ and $z = -d$, it can be deduced that

$$\mathcal{E}_{ff} = \frac{(1 - |\Gamma_m(0^-)|^2)(1 - |\Gamma_1(-d^-)|^2)e^{-2\alpha_m d}}{1 - |\Gamma_m(0^-)e^{-2\alpha_m d}|^2} \tag{14}$$

Then, this result can be rewritten for the particular case of the lossless lambda quarter impedance transformer [15], [29] in which $\eta_m = \sqrt{\eta_1 \eta_2}$ and $d = \lambda_m/4$. Under these conditions, it is expected to obtain $|\Gamma_1(-d^-)|^2 = 0$ and if $\alpha_m = 0$, then there is a maximum transfer of density power of Medium 1 to Medium 2, it means $\mathcal{E}_{ff} = 1$. Therefore, the Fig. 3 configuration can be utilized to match Medium 1 and Medium 2. Nevertheless, it is necessary to design a material with the desired η_m and α_m values in order to implement this kind of solution.

3) The Problem of the Inefficient Transfer of Power from Air to some Materials Associated to the Described Applications: Most non-metallic materials used in various microwave applications are poor conductors, non-magnetic ($\mu' \to \mu_0$), and polarizable ($\epsilon' > \epsilon_0$) for $\epsilon'' \to 0$. Examples include cement which can be an obstacle in telecommunication links [30], while wood, oil, paper, rubber, glass, water, food and soil are involved in microwave heating applications [31], [32], [33]. On the other hand, human tissues are involved in biomedical microwave tomography and radiometry applications [11], [12], [34]. Since these materials exhibit $\mu' \to \mu_0$ and $\epsilon' > \epsilon_0$, the real part of their intrinsic impedance, denoted as $\Re(\eta)$, is lower than that of air ($\eta_0 \approx 377\ \Omega$). In fact, $\Re(\eta)$ diminishes as the moisture content in the material increases, according to the literature [33]. For example, distilled water has one of the lowest intrinsic impedance values among these materials ($\approx 43\Omega$), meaning that only about 36 percent of the incident wave's power density can be transmitted from air to distilled water in the microwave band for normal incidence (see Eqations (8) and (9)).

B. Modeling a Metamaterial Suitable for Volumetric Impedance Matching Systems

Metamaterials are engineered artificial mediums made up of arrays of cells composed of conductive and dielectric materials. The value of the resultant metamaterials macroscopic electromagnetic parameters, ϵ and μ, are often difficult to obtain with natural materials. Due to their exotic properties and potential for reconfigurability, metamaterials have found applications in optics and radiofrequency [26], [35]. However, despite their potential, the design of metamaterial-based matching systems aimed at increasing power transfer from a plane wave through a plane interface remains a relatively underexplored topic. Some metasurfaces designed for heating applications require specialized manufacturing processes for ceramic materials and lack reconfigurability [19], [20], [21]. Others may exhibit anisotropy and their electromagnetic behavior has not been completely studied [23].

In response to these gaps, in this paper a cubic conductors metamaterial with low attenuation, simple geometry, isotropic behavior, and dynamic reconfiguration capabilities is analytically modeled and utilized to match two different media. A representation of this metamaterial is shown in the Fig. 3.

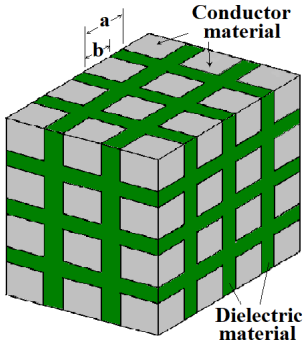

Fig. 3. Cubic conductors metamaterial bulk.

1) Analytical Model: Previous studies represented the electric permittivity ϵ_m and magnetic permeability μ_m values of the cubic conductor metamaterial as functions of the metamaterial's geometric dimensions in [24], [25]. These representations seem to be good approximations when losses are negligible, when edge field effects inside the metamaterial are minimal, and when the length of the cubic cell is much smaller than the wavelength λ. This model demonstrates the metamaterial's capability to restrict magnetic field flow within the medium while simultaneously polarizing it. It establishes that ϵ_m and μ_m can be approximated as: $\epsilon_m \approx \epsilon' \approx \epsilon_d/(1 - b/a)$ and $\mu_m \approx \mu' \approx \mu_0 \left(1 - (b/a)^2\right)$ for a non-magnetizable dielectric, where b is the edge length of the conductor cube inside the cubic cell, a is the length of the cubic cell (with $a > b$), while ϵ_d and μ_d are the parameters of the dielectric material between the conductor cubes. From the analysis carried out using this model, it can be concluded that $\epsilon_m > \epsilon_0$ and $\mu_m < \mu_0$, since for common dielectric insulators occurs that $\epsilon_d \geq \epsilon_0$ and $\mu_d \approx \mu_0$. This results in a metamaterial impedance intrinsic value which complies with $\Re(\eta_m) < \eta_{air}$, where $\eta_{air} \approx \sqrt{\mu_0/\epsilon_0}$. On

the other hand, most target substances that must propagate and/or absorb radiation, represented as Medium 2 in Fig. 2 (e.g., water, wood, glass, etc.), also show a real part of their intrinsic impedance that is lower than that of vacuum, since $\mu_2 \approx \mu_0$ and $\Re(\epsilon_2) > \epsilon_0$ [29], [31]. Therefore, the metallic cubic conductor metamaterial proposed in this work is suitable as an impedance matching medium between air and these substances, given that both the target substances and the metamaterial exhibit intrinsic impedances within the same range of values.

In spite of the studies developed in [24], [25], the metallic cubic conductor metamaterial has aspects that have not been fully explored. Its intrinsic losses and its behavior's dependence on the operation frequency are among these important parameters for designing an impedance matching system. Consequently, to investigate these aspects, the metamaterial behavior is represented by the quasi-static Drude-Lorentz homogenization model described in [35], conceived for cases where the metamaterial cell size is much smaller than the operation wavelength. The metamaterial cell is modeled as a circuit to derive both ϵ_m and μ_m as functions of the operation frequency and of the circuit parameters associated to the metamaterial cell (see Fig. 4). According to the model,

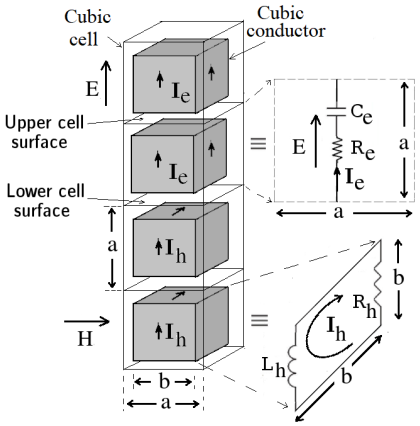

Fig. 4. Circuit elements related to the Drude-Lorentz model for the proposed metamaterial.

the cell circuit parameters C_e and R_e represent the interaction of the metamaterial cell with an incident low frequency electric field **E** that generates a displacement current and a conduction current in the cell in the same direction of **E**. The average of these vertical induced currents in the metamaterial cell is denoted as the net current I_e which is related to the average displacement current in the cell by the relation $I_e/a^2 = j\omega\epsilon_m \mathrm{E}_0$, being E_0 the average electric field in the cell and being ϵ_m the effective metamaterial electric permittivity. Then, the difference of potential $\mathrm{E}_0 a$ between the upper and lower surfaces that limit the metamaterial considered cell is $\mathrm{E}_0 a = (R_e + (j\omega C_e)^{-1})I_e$ (see Fig. 4). Then, after performing the necessary algebraic manipulations, ϵ_m can be defined as

$$\epsilon_m \approx \frac{1}{j\omega a(R_e + (j\omega C_e)^{-1})} \tag{15}$$

where C_e is the capacitance that exists between the upper and lower surfaces of a^2 area that limit the considered metamaterial cell (see Fig. 4), which in this case is approximately $C_e \approx \epsilon_d a^2/(a-b)$. Then, R_e is assumed to be the equivalent resistance between the upper and lower sides of the conductor cube, resulting from the parallel arrangement of the four individual resistances corresponding to each of vertical square conductor volumes through the laminar current I_e flows. In each one of these volumes, it is assumed that I_e flows through a thin slab whose transverse area is $b\delta_c$, on a vertical path whose length is b. These assumptions lead to the proposal that $R_e \approx 1/(4\sigma_c\delta_c)$, being δ_c and σ_c the skin depth and the conductivity of the cubic conductor material respectively, assuming that $\delta_c << b$.

On the other hand, the circuit parameters L_h and R_h in the considered cell of Fig. 4 represent the interaction of the metamaterial cell with a low-frequency magnetic field that induces a conduction current I_h in the cubic conductor of the cell, when $\mu_d \approx \mu_0$. The Faraday's Law establishes a relationship between I_h and the induced magnetic flux inside the conductor cube. The induced magnetic flux can be defined as the flux of the induced density magnetization field **M** through the cube's transverse surface of area b^2, bounded by the four side conductor cube walls parallel to the incident magnetic field $\mathbf{H} = \mathrm{H}_0\hat{\mathbf{h}}$ which has the same magnitude and opposite direction to **M** inside the conductor cube, stablishing that $\mathbf{M} = \mathrm{M}_0\hat{\mathbf{m}}$ only inside such conductor. Using the integral form of the Faraday's Law, we propose that $-j\omega b^2\mu_0\mathrm{M}_0 = (R_h + j\omega L_h)I_h$, where the term $(R_h + j\omega L_h)I_h$ represents the electromotive force induced in the solenoid of the four cube conductor faces considered in this calculation. On the other hand, it is necessary to define the amplitude of the average cell density of magnetization in the cell $\bar{\mathbf{M}}$ which is by definition the ratio between the cell magnetic dipolar moment $I_h b^2$ and the cell volume whose value is a^3, what yields to write that $\bar{\mathbf{M}} = -I_h(b^2/a^3)\hat{\mathbf{m}}$ [36]. Moreover, $\bar{\mathbf{M}}$ is also related to the average incident magnetic field by the relation $\bar{\mathbf{M}} = (\frac{\mu_m}{\mu_0} - 1)\bar{\mathbf{H}}$ [36], where $\bar{\mathbf{H}} = \mathrm{H}_0\hat{\mathbf{h}}$ for the considered cell. This analysis enables us to derive the effective metamaterial magnetic permeability μ_m as follows, after performing several algebraic manipulations

$$\mu_m \approx \mu_0\left(1 - \frac{j\omega\mu_0 b^4}{(R_h + j\omega L_h)a^3}\right) \tag{16}$$

where L_h is the approximated value of the inductance associated with the conduction current I_h flowing through the solenoid formed by the four conductor cube faces that are parallel to **H**, while R_h is the resistance associated with this coil. L_h represents the inductance of the cubic solenoid with a transverse surface area of b^2 and a magnetic permeability of μ_0 value, with the solenoid height fixed at a because a magnetic significant coupling with the adjacent cells has been assumed. Hence, we propose that $L_h \approx \mu_0 b^2/a$. Then, R_h is the sum of the four individual resistances corresponding to each one of the four solenoid conductor square thin slabs in which the current I_h flows. For each one of such volumes, I_h flows through a transverse area of $b\delta_c$ whose length is b,

being $4b$ the total coil lenght path. Hence, it is also proposed that $R_h = 4/(\sigma_c \delta_c)$.

Finally, note that Equations (15) and (16) take respectively the forms of ϵ_m and μ_m used in [25] when losses are negligible and the operation frequency is sufficiently low, which occurs when $\omega \to 0$, $R_e \to 0$ and $R_h \to 0$.

2) Metamaterial Symmetry and Periodicity Properties: Metamaterials present useful features that can simplify their FDTD simulation, such as axial symmetry and periodicity [37], [38]. For the case of the cubic conductor metamaterial, these properties are illustrated in Fig. 5.a, where a representation of the infinite cubic conductor metamaterial fields is shown, assuming a normal incidence problem in which the incident wave's electric and magnetic fields are parallel to different metamaterial axes. In this figure, it can be observed that the electric field is normal to the cell's upper and lower boundary surfaces and parallel to the cell's side boundary surfaces. Similarly, the magnetic field is normal to the cell's side boundary surfaces and parallel to the cell's upper and lower boundary surfaces.

By taking advantage of these symmetry and periodicity properties, the infinite metamaterial propagation problem in Fig. 5.a can be simplified to a finite one by redefining the cell boundaries, as shown in Fig. 5.b. In this scheme, it is ensured that the electric field is normal to the added perfect electric conductor (PEC) surfaces of the upper and lower cell boundaries and parallel to the added perfect magnetic conductor (PMC) surfaces of the cell's side boundaries. Likewise, the magnetic field is parallel to the added PEC upper and lower boundary surfaces and normal to the added PMC side boundary surfaces.

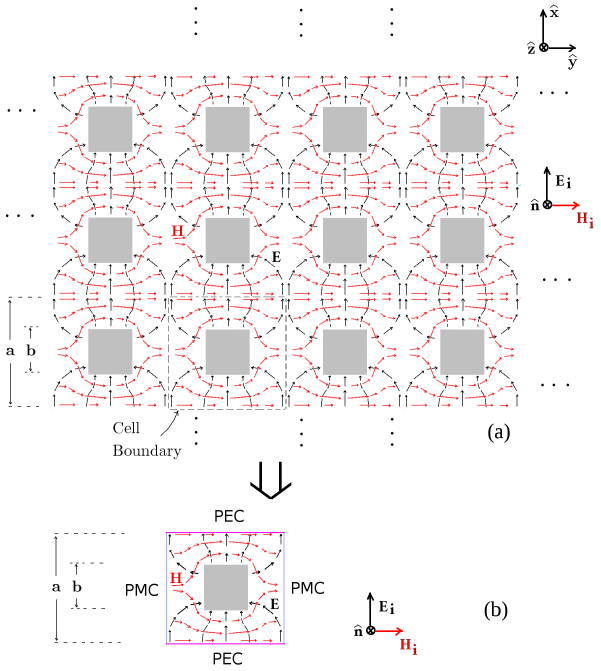

Fig. 5. Metamaterial traverse cut and fields: (a) Infinite medium. (b) Simplified model.

III. Test Scenarios

In this section, both the behavior of the metamaterial parameters and the performance of a metamaterial-based impedance matching system are studied. These analyses were conducted using both numerical simulations and analytical methods in the described scenarios.

A. Metamaterial Constitutive Parameters and Intrinsic impedance

In this section, the ratios ϵ'_m/ϵ_0 and μ'_m/μ_0 were computed using the student version of Ansys-HFSS software, employing a local homogenization approach. For this estimation, a perfect conductor cube with an edge length b was chosen for the metamaterial, with air as the insulating material between the cubes. The estimation was carried out using the symmetry properties illustrated in Fig. 5.

The ratio ϵ'_m/ϵ_0 was estimated using a cubic cell of size $a = 2.4$ cm, as shown in Fig.6.a, where the upper and lower faces are both perfect electric conductor (PEC) surfaces, and the four side faces are perfect magnetic conductor (PMC) surfaces. In this scenario, the capacitance between the two PEC surfaces was estimated with Ansys-HFSS software twice. First, in the absence of the conductor cube to obtain C_0 and then, in the presence of the conductor cube to obtain C_m. The ratio ϵ'_m/ϵ_0 is equivalent to the ratio C_m/C_0 [38]. Using this procedure, the ratio ϵ'_m/ϵ_0 was computed for each one of the selected 24 equally spaced values of b/a. The obtained results are presented in Fig. 7.

The ratio μ'_m/μ_0 was estimated using a cubic cell of size $a = 2.4$ cm, as shown in Fig. 6.b, where the upper and lower faces are both perfect magnetic conductor (PMC) surfaces, and the four side faces are perfect electric conductor (PEC) surfaces. In this scenario, the inductance associated with the magnetic flux that traverses the two PMC surfaces was estimated with Ansys-HFSS software twice. First, in the absence of the conductor cube to obtain L_0 and then, in the presence of the conductor cube to obtain L_m. The ratio μ'_m/μ_0 is equivalent to L_m/L_0. Using this procedure, the ratio μ'_m/μ_0 was computed for each of the selected 24 equally spaced b/a values. The obtained results are presented in Fig. 8.

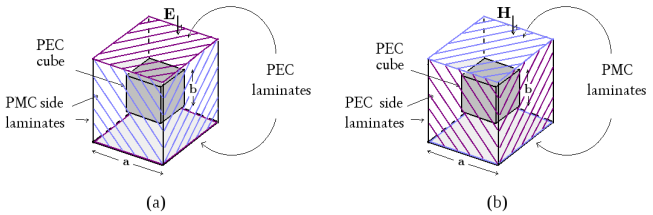

Fig. 6. Cells utilized for the constitutive parameters estimation. (a) For ϵ'_m/ϵ_0 ratio. (b) For μ'_m/μ_0 ratio.

Next, one of the most important metamaterial parameters for the impedance matching system design, $\Re(\eta_m)$, was estimated using the relation $\eta_m \approx \Re(\eta_m) \approx \sqrt{\mu'_m/\epsilon'_m}$, which is valid for low-loss media. This was done using the simulation data from Figs. 7 and 8, and the results are presented in Fig. 9. The parameter $\Re(\eta_m)$ was also calculated analytically using

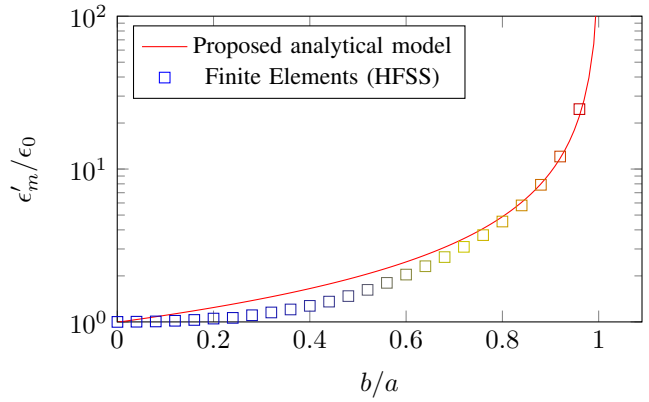

Fig. 7. Metamaterial relative electric permitivity given by ϵ'_m/ϵ_0 as a function of b/a.

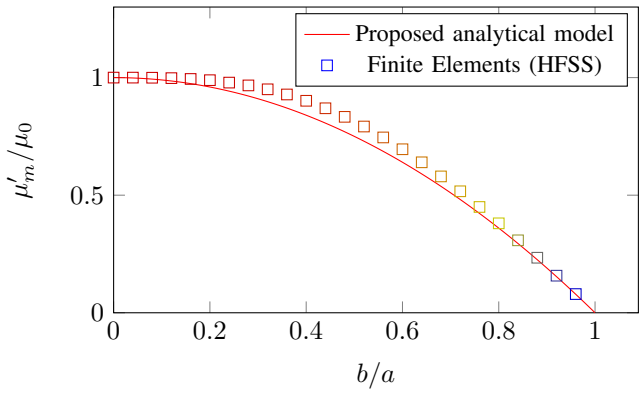

Fig. 8. Metamaterial relative magnetic permeability given by μ'_m/μ_0 as a function of b/a.

the proposed model, based on Equations (15) and (16), and the results are also presented in Fig. 9.

B. Metamaterial Attenuation Constant

Another important metamaterial parameter for the impedance matching system design is α_m, which is estimated and calculated in the following test scenario. Aluminum conductor cubes with the following properties were chosen for the metamaterial: $\epsilon_{Al} = \epsilon_0$, $\mu_{Al} = \mu_0$, and $\sigma_{Al} = 3.8 \times 10^7$ S/m, while air was used as the insulating material between the cubes. The chosen cell length for these tasks was $a = \lambda_0/50 = 2.45$ mm, where $\lambda_0 = c/f_0$ for $f_0 = 2.45$ GHz. For this f_0, a known good conductor approximation was assumed for δ_{Al} [29], which yields $\delta_{\mathrm{Al}} = (\pi f_0 \mu_{\mathrm{Al}} \sigma_{\mathrm{Al}})^{-1/2} = 1.657$ μm. Then, α_m was analytically calculated using the proposed homogenization model given by Equations (3), (15), and (16). α_m was also estimated numerically using an FDTD algorithm in the simulation scenario presented in Fig. 10.b, which is a waveguide equivalent to the infinite dimensions scenario in Fig. 10.a. The waveguide is limited by PEC upper and lower side walls, with PMC lateral walls, and is filled with air for $z < 0$ and metamaterial for $z > 0$. A transverse electromagnetic (TEM) wave propagates in the $\hat{z}$ direction within the air medium. Two probes were placed at the central metamaterial axis, as indicated in Fig. 10.c, at positions $z = d_1 = \lambda_0/6$ and $z = d_2 = 5\lambda_0/18$, to obtain the electric field amplitudes $|\mathbf{E}(d_1)|$ and $|\mathbf{E}(d_2)|$. These values are used to determine α_m through the relation $\alpha_m = \frac{1}{d_2 - d_1} \ln\left(\frac{|\mathbf{E}(d_1)|}{|\mathbf{E}(d_2)|}\right)$. The results for α_m as a function of the ratio b/a are presented in Fig. 11.

C. Metamaterial Impedance Matching Application

Moreover, the impedance matching application scenario of the Fig. 12 was also simulated in order to show the practical importance of this work, where the Medium 1 is air with parameters $\epsilon_1 = \epsilon_0$, $\mu_1 = \mu_0$, $\sigma_1 = 0$ and Medium 2 represents water with some salts dissolved, such as $\epsilon_2 = \epsilon_0$, $\mu_2 = \mu_0$, $\sigma_2 = 0.7$ S/m, being $\eta_1 = 377\Omega$ and $\eta_2 \approx 42\Omega$.

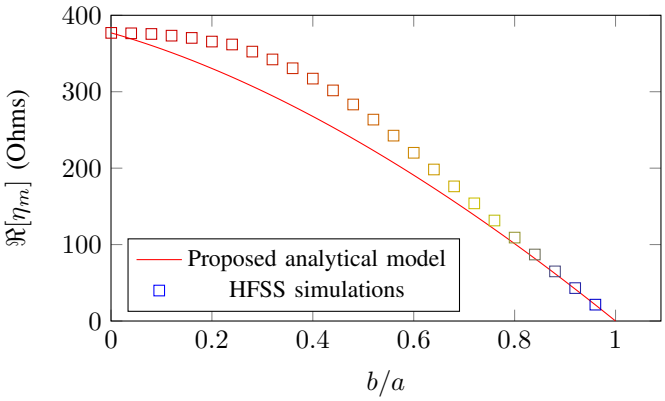

Fig. 9. Real part of the intrinsic impedance of the cubic conductor metamaterial as a function of b/a ratio, for f=2.45 GHz and a=2.44 mm.

A lambda quarter transformer slab constructed with the cubic conductors metamaterial is added between volumes of air and water. Aluminum conductor cubes of $\epsilon_{Al} = \epsilon_0$, $\mu_{Al} = \mu_0$, and $\sigma_{Al} = 3.8 \times 10^7$ S/m were chosen, while air was used as the insulator between the metamaterial cubes. The chosen width of the metamaterial lamdda quarter transformer slab is such that $d = Na \approx \lambda_m/4$, for the cells edge size fixed in $a = 2.45$mm, being $N = 10$ and $b/a = 0.75$. Then, the efficiency of the transferred density power from the Medium 1 to the Medium 2, let $\mathcal{E}_{ff}$, is calculated by means of the Equation (14) utilizing the relations $\alpha_m = \Re(\gamma_m) = \Re[j\omega\sqrt{\epsilon_m \mu_m}]$ and $\eta_m = \sqrt{\mu_m/\epsilon_m}$ where μ_m and ϵ_m are the given by the proposed model represented by Equations (16) and (15) respectively. $\mathcal{E}_{ff}$ was also estimated numerically through an analysis of the standing wave pattern obtained from an FDTD simulation of the scheme in Fig. 12.b, which is a guidewave equivalent to the infinite dimensions scenario in Fig. 12.a. The guidewave is limited by PEC upper and lower side walls and PMC lateral walls. It is filled with air for $z < -d$, with metamaterial for $-d < z < 0$, and with water for $z > 0$. The waveguide is excited with a transverse electromagnetic (TEM) wave propagating in the $\hat{z}$ direction. A probe is located at the center of the metamaterial axis, at $z = d_1 = 31$ mm, to measure the average electric field amplitude $|\mathbf{E}(d_1)|$. This

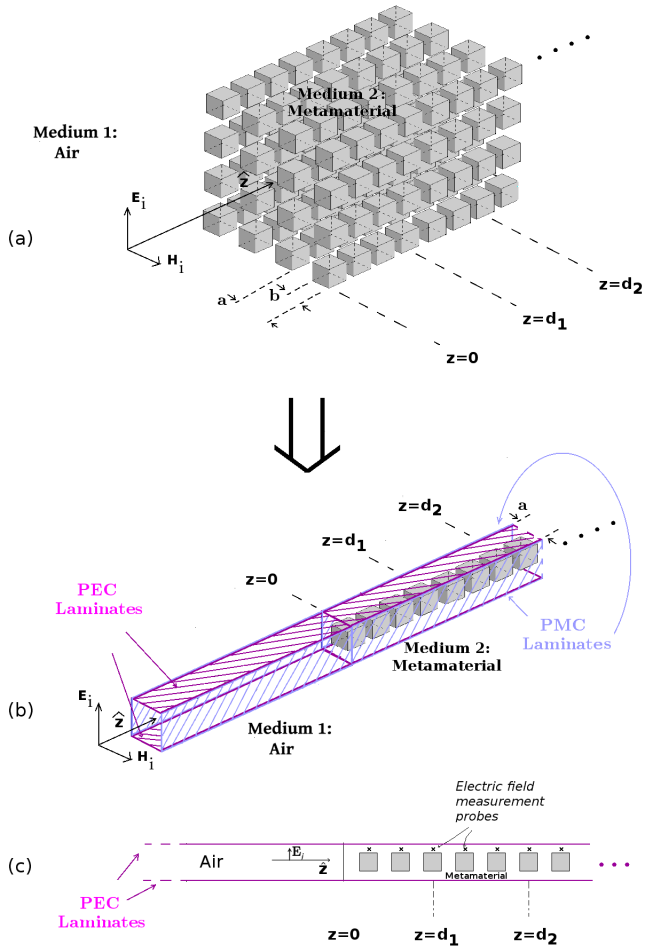

Fig. 10. Normal incidence problem with an air-metamaterial interface. (a) Theoretical case of mediums with infinite dimensions. (b) Equivalent simulation guidewave for the attenuation constant α_m estimation. (c) Traverse cut of the simulation guidewave and location of the electric field probes.

value is used to determine $\mathcal{E}_{ff}$, and the results are shown as a function of the operating frequency f_0 in Fig. 13.

IV. Results and Discussions

Good agreement is observed between analytically and numerically obtained metamaterial parameters in Figs. 7, 8 and 9. It can be observed in Fig. 9 that the metamaterial intrinsic impedance real part decreases with the b/a ratio. By contrast, according to the results shown in Fig. 11, the metamaterial attenuation increases with the b/a ratio. The maximum value obtained for α_m is around 1 Np/m in the chosen test scenarios, which is significantly lower than the corresponding values for matching liquid solutions, which can exhibit attenuations of up to 15 dB/cm [16]- [18]. The reflection coeficient in Medium 1 ($|\Gamma_1|$) and the power transfer efficiency $\mathcal{E}_{ff}$ from air to water without a matching system are respectively $|\Gamma_1| = 0.80$ and 36% (see Section II-A3), but these values improve respectively to 87% and $|\Gamma_1| = 0.36$ for f_0=2.45 GHz when the designed matching system is implemented at the interface (see Fig. 13).

According to [39], there is a minumun acceptable impedance matching for radiant systems if the field standing

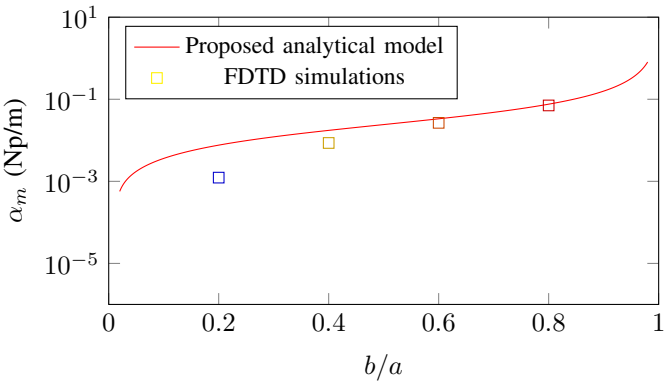

Fig. 11. Attenuation constant α_m of the cubic conductor metamaterial as a function of b/a ratio, for f=2.45 GHz and $a = 2.45$mm.

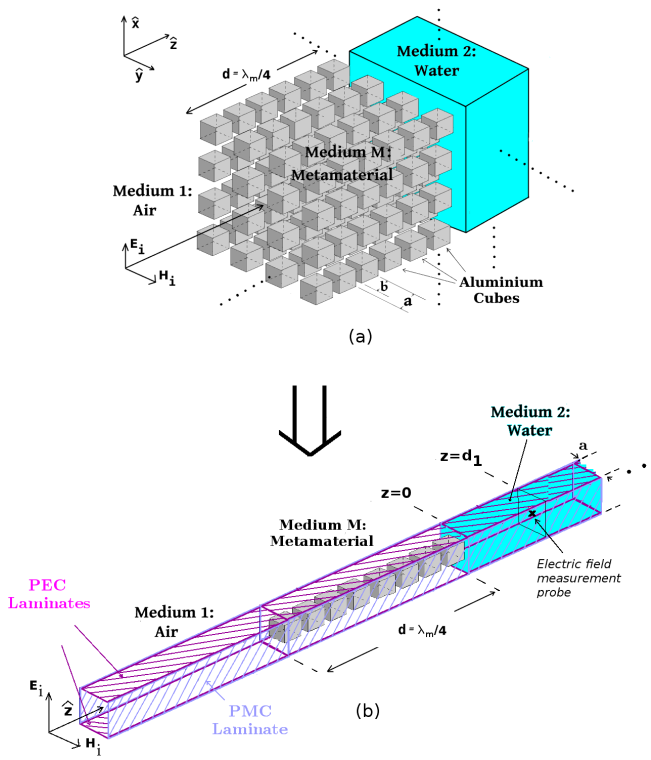

Fig. 12. Lambda quarter impedance air-water transformer based on a metamaterial of metallic cubic conductors, for a plane interface and normal incidence.(a) Theoretical case of mediums with infinite dimensions. (b) Equivalent simulation guidewave for the power system efficiency estimation.

wave ratio (SWR) complies with the condition SWR < 3, which occurs when at least 75% of the incident wave power is transfered to the target medium. Using this reference, the obtained system bandwidth for the studied scenario of the Fig. 12 is between 1.99 GHz and 3.07 GHz (see Fig. 13), according to the realized simulations.

The slight discrepancies between the analytical and numerical results shown in Figs. 9, 11, and 13 may be attributed to edge effects of the electric and magnetic fields around the edges of the metallic cubes, which were not accounted for in the circuit parameter estimations from the

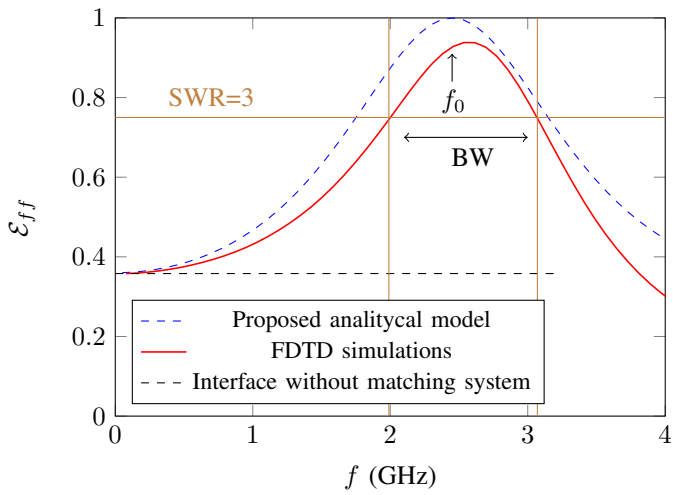

Fig. 13. Power transfer efficiency $\mathcal{E}_{ff}$ from air to water for the proposed matching system of Fig.12 as a function of the operation frequency f.

proposed model represented by Equations (15) and (16). However, these effects are minimized as b/a ratio approaches either 0 or 1, as evidenced in Fig. 9. Furthermore, the model may lose accuracy if the edge length a is not sufficiently small relative to λ_0, particularly at higher frequencies where non-desired evanescent reactive propagation modes might arise in the metamaterial, as observed in Fig. 13.

Despite the possible presence of these effects, the model represented by Equations (15) and (16) provides a good approximation for several under-explored aspects of the metamaterial behavior, like its attenuation, intrinsic impedance, and bandwidth.

V. Conclusions

In this work, a cubic conductor cell metamaterial is proposed as a impedance matching medium, introducing a novel technique for efficiently transferring electromagnetic plane wave power between volumetric media, being the involved materials similar to those typically used in microwave heating, biomedical systems, and telecommunications applications. An analytical model based on the Drude-Lorentz homogenization method was developed to predict metamaterial behavior, incorporating operation frequency and ohmic losses, which are not adressed in previous models [24], [25]. Numerical simulations demonstrated strong agreement with the proposed analytical model, showing significantly lower metamaterial losses compared to impedance-matching liquid solutions [16], [17], [18]. The metamaterial also offers a wide range of values for its intrinsic impedance being its real part, between zero and 377Ω, confirming its versatility for different application scenarios. These improvements were achieved using low-cost materials instead of high-permittivity ceramics [19], [20], [21]. The studied application case highlighted the design of a metamaterial-based quarter-wavelength impedance transformer for matching air and water, improving power transfer efficiency from 36% to 87% at the air-water interface due to the implementation of the designed matching system.

VI. Acknowledgements

Stimulating discussions with the professors Diogenes Marcano and Monica Huerta aiming to focus and develop this work are gratefully acknowledged by the authors. The authors also would like to thank Chat GPT for its assistance in proofreading and editing this manuscript. The AI tool helped identify and correct errors in grammar, spelling, and punctuation. However, the authors also conducted a thorough manual review to ensure the accuracy and clarity of the content.

References

[1] B. L. Hayes , “Microwave Synthesis - Chemistry at the Speed of Light”, *CEM Publishing*, North Carolina, USA, 2002. ISBN: 978-097-22-2290-7.

[2] M. Cann, “Microwave Heating as a Tool for Sustainable Chemistry”, *CRC Press*, Florida, USA, 2010. ISBN: 978-143-98-1270-9.

[3] T. Abo Bakr, “Microwave Applications in Food Processing: An Overview,”. *Alexandria Journal of Food Science and Technology*, vol 17, no. 2, pp. 11-22, 2020. doi: 10.21608/ajfs.2020.150658 .

[4] W. Cao, “The development and application of Microwave Heating”, *InTech*, 51000 Rijeka Croatia, ISBN 978-953-51-0835-1, 2012. http://dx.doi.org/10.5772/2619.

[5] O. Kharissova, B. Kharisov and J. J. Ruiz, “Review: The use of microwave irradiation in the processing of glasses and their composites,” *Industrial and Engineering Chemistry Research*, vol. 49, no. 4, pp. 1457-1466, 2010. https://doi.org/10.1021/ie9014765

[6] D.A. Jones et al, “Microwave heating applications in environmental engineering: A review,” *Resources, Conservation and Recycling*, vol. 34, pp. 75-90, 2002. DOI: https://doi.org/10.1016/S0921-3449(01)00088-X .

[7] S. Mutyala et al, “Microwave applications to oil sands and petroleum: A review”, *Fuel Processing Technology*, vol. 91, pp. 127-135, 2010. DOI: 10.1016/j.fuproc.2009.09.009 .

[8] I. L. Boshkova et al, “Perspective of using microwave heating of petroleum products in the tank”, *JNTES*, vol. 4, pp. 127-135, 2021. DOI: 10.53412/jntes-2021-4-4.

[9] F. Mascarenhas, A. Dias, and A. Christoforo, “State of the Art of Microwave Treatment of Wood: Literature Review” *Forests*, vol 12, no. 6, pp. 745. 2021. https://doi.org/10.3390/f12060745

[10] J. Krouzek and et al, “Pilot scale applications of microwave heating for soil remediation,” *Chemical Engineering and Processing - Process Intensification*, vol. 130, pp. 53-60, 2018. https://doi.org/10.1016/j.cep.2018.05.010

[11] S. Raghavan, “Metamaterials in Medicine” in: *Handbook of Metamaterial-Derived Frequency Selective Surfaces*. Springer Nature Singapore. pp. 623-642. 2022. DOI: https://doi.org/10.1007/978-981-16-6441-0_22

[12] N. A. Jaffar et al, “An overview of metamaterials used in applicators in hypertermia cancer treatment procedure”, *2017 International Conference on Electrical, Electronics and System Engineering (ICEESE)*, Japan, 2017. pp. 32-36 DOI: 10.1109/ICEESE.2017.8298389.

[13] Z. Zhang et al, “Wireless Power Transfer - An Overview,” *IEEE Transactions on Industrial Electronics*, vol. 66, no. 2, pp. 1044-1058, 2019. DOI: 10.1109/TIE.2018.2835378.

[14] M. Wu et al,“Development and Prospect of Wireless Power Transfer Technology Used to Power Unmanned Aerial Vehicle” *Electronics*, vol. 11, 1389, 2022, https://doi.org/10.3390/electronics11152297 .

[15] K. Wu, L. Zhu and R. Vahldieck “Microwave Passive Components” in “Chapter 7 of: Microwave Circuits - An Overview”, *Elsevier*, 2005. pp. 592-593, DOI:10.1016/B978-012170960-0/50044-X

[16] P. M. Meaney, C. J. Fox, S.D. Geimer and K. P. Paulsen, “Electrical Characterization of Glycerin: Water Mixtures: Implications for Use as a Coupling Medium in Microwave Tomography,” *IEEE Trans. Microw. Theory Tech.*, May 2017. 65(5):1471-1478. 2017. doi: 10.1109/TMTT.2016.2638423.

[17] W. Shao and B. Zhou,"Effect of Coupling Medium on Penetration Depth in Microwave Medical Imaging", *Diagnostics*. 12, 2906, 2022. DOI: 10.3390/diagnostics12122906
[18] V. Hamsakutty et al,"Coupling medium for microwave medical imaging applications", *Electronic Letters*, vol. 39, Nº 21, 2003. DOI: 10.1049/el:20030979
[19] Q. Chen et al,"High-efficiency microwave heating method based on impedance matching technology", *AIP Advances*. 9, 015113. 2019. doi:10.1063/1.5065410
[20] F. Yang et al, "Continuous-Flow Microwave Reactor for High-Performance Heating of a Dynamic Chemical Reaction System", *Ind. Eng. Chem. Res.*. 19459-19470, 62, 2023. DOI:10.1021/acs.iecr.3c03294
[21] F. Yang et al, "High-Efficiency Continuous-Flow Microwave Heating System Based on Asymmetric Propagation Waveguide", *IEEE Transactions on Microwave Theory and Techniques*, Vol. 70, Nº. 3, March 2022. DOI: 10.1109/TMTT.2021.3123400
[22] A. Moradpour et al,"Development of a Solid and Flexible Matching Medium for Microwave Medical Diagnostic Systems", *Diagnostics*. 11, 550, 2021. DOI:10.3390/diagnostics11030550
[23] Z. Wu et al, "Highly efficient microwave heating for target area based on metamaterial", *Microwave and optical technology letters*, vol. 59, no. 4, pp. 758-761, 2017. DOI: 10.1002/mop .
[24] B. Wood and J. B. Pendry, "Metamaterials at zero frequency," *J. Phys.: Condens. Matter*, vol. 19, no 7, p. 076208. 2007. doi: 10.1088/0953-8984/19/7/076208.
[25] P. Belov *et al.*, "Broadband isotropic μ-near-zero metamaterials," *Applied Physics Letters*, vol. 103, no 21, p. 211903, November, 2013. doi: 10.1063/1.4832056
[26] J. P. Turpin et al,"Reconfigurable and Tunable Metamaterials: A Review of the Theory and Applications", *International Journal of Antennas and Propagation*. 429837, 2014. https://doi.org/10.1155/2014/429837
[27] C. Balanis, "AC Variations in Materials" in *Advanced Engineering Electromagnetics*, NY, USA: Wiley, 1989, ch. 2, sec. 2.8, pp. 72-85. ISBN: 0-471-62194-3
[28] J. D. Jackson , "Classical Electrodynamics", *John Wiley and Sons*, Second Edition. New York. 1962. ISBN: 0-471-43132-X .
[29] S. Marshall, "Electromagnetismo, conceptos y aplicaciones", *Prentice Hall Hispanoamericana*, 1997, Estado de México, México. ISBN 968-880-954-3.
[30] J. De Frutos, L. Soler y C. Andrade, "Propiedades dieléctricas de pastas de cemento con reducido contenido de agua libre," *Boletín de la Sociedad Española de Cerámica y Vidrio*, vol. 38, no. 6, pp. 607-610, Dic. 1999. http://hdl.handle.net/10261/15070
[31] M. Kraus "Electro-magnetismo", *Mc Graw Hill*, 3º Edición, 1992. ISBN: 968-451-842-0. pp. 815.
[32] M. Sadiku "Elements of Electromagnetics", *Oxford University Press*, 2001. , ISBN 0-19-513477-X. pp. 737-738.
[33] M. Vollmer, "Physics of the microwave oven", *Physics Education*, vol. 39, no 1, pp. 74-81, 2004. DOI: 10.1088/0031-9120/39/1/006
[34] P. Hasgall et al, "IT'IS Database for thermal and electromagnetic parameters of biological tissues", Version 4.1. Feb. 22, 2022. DOI: 10.13099/VIP21000-04-1. www.itis.swiss/database
[35] R. Barroso and W. Malpica, "An Overview of Electromagnetic Metamaterials," *IEEE Lat. Am. T.*, vol. 18, Iss. 11, pp. 1862-1873, Nov., 2020. DOI: 10.1109/TLA.2020.9398627
[36] M. Kraus "Electro-magnetismo", *Mc Graw Hill*, 3º Edición, 1992. ISBN: 968-451-842-0. pp. 235-240.
[37] A. J. Kogon and C. D. Sarris, "FDTD Modeling of Periodic Structures: A Review," *Physics.comp-ph*, arXiv:2007.05091, Aug. 2020. DOI:10.48550/arXiv.2007.05091
[38] D. Smith, "Metamaterials — Basic Homogenization," people.ee.duke.edu https://people.ee.duke.edu/drsmith/metamaterials_homogenization.htm (accessed Febraury 03, 2025).
[39] H. Shantz "The Art and Science of Ultrawideband Antennas", *Artech-House*, 2005. ISBN: 1-58053-888-6. pp. 235-240. Chapter 2. pp 62.

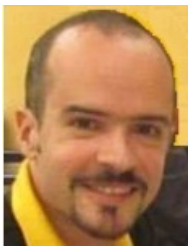

Raul Horacio Barroso Salcedo received his Bachelor and his M.Sc. degrees in Electrical Engineering from the Central university of Venezuela in 2000 and 2009 respectively. Currently, he is also pursuing his Ph.D. metamaterial studies in the Faculty of Engineering of the Central University of Venezuela, and he is just a Ph.D. candidate. Since 2006 he has been a full professor in the Simon Bolivar University in Venezuela and he is currently hired there as an associated teacher. His research interests include metamaterials, fractal antennas, multiband antennas, broadband antennas, and analysis and design of broadband matching systems. Raul Barroso has published an overall of ten IEEE and IET articles as a main author in these areas.

Wilmer Napoleón Malpica Albert is an Electrical Engineer and full professor from the Faculty of Engineering of the Central University of Venezuela. He pursued his P.h.D studies in the Technical university of Lisbon. Currently, he is a researcher in the applied electromagnetism area, specially in the theory and application of grounding systems.

Alfonso Zozaya received his B.Sc. degree in Electronic Engineering, with a major in Telecommunication, from the Instituto Universitario Politécnico de las Fuerzas Armadas Nacionales de Venezuela (I.U.P.F.A.N.), Maracay, Venezuela, in 1991, and his PhD degree from the Universidad Politécnica de Cataluña (UPC), Barcelona, Spain, in the area of Signal Theory and Communications in 2002. He worked as a Professor at the University of Carabobo, Valencia, Venezuela from 1994 to 2014. Currently, he is Full Professor in the Departamento de Electricidad at the Universidad Tecnológica Metropolitana (UTEM), Santiago de Chile. His research areas of interest are applied electromagnetic, computational electromagnetic, digital signal processing, RF circuits design, synthetic aperture radars, and impulsive UWB radars.